

Interface for Semi-automatic Image Contrast Enhancement in the Propagation-based X-ray Phase Contrast Method

A.V. Polishchuk^{1,*}, M.O. Pavlyuk^{1,2}, A.V. Tarasenko², V.V. Zhurakulov²

¹ Institute of Applied Physics of the National Academy of Sciences of Ukraine, 58, Petropavlivska Str., 40000 Sumy, Ukraine

² Sumy State University, 2, Rymky Korsakov Str., 40007 Sumy, Ukraine

(Received 06 March 2023, revised manuscript received 17 August 2023, published online 30 August 2023)

This paper describes a graphical user interface developed for the normalization of radiograms and semi-automatic search for the most contrast images using a given reference, the experimental data for which were obtained using the analytical technique of X-ray phase contrast imaging. The projections of the biological object were obtained by applying free space propagation of coherent radiation when no additional optical elements are placed between the sample and the detector equipped with a YAG:Ce scintillator to exploit the interference effects characteristic of the method due to the high-intensity characteristics of the X-ray light of the SOLEIL synchrotron. The energy of the X-ray photons was 10 keV, and the distance between the sample and the detector was 16.5 cm. We consider the use of standard Matlab tools for algorithmic correction of inhomogeneities of the detector and probing light beam used to build an image of the internal structure of the object and to evaluate the contrast of a group of images, by choosing such common quality criteria as PSNR and SSIM. The program is able to generate such a set of images depending on the parameters entered by the user for a subjective search for contrast images. Numerical estimates well confirm the visual results of the algorithmic search and allow us to reach the most informative image from the generated array, which is created by the user using the interface. The aim of this work is to familiarize with the use of the developed software product and the concept of semi-automatic search among the dataset of digital phase-contrast images.

Keywords: Matlab, Semi-automatic, Interface, Normalization, X-ray phase-contrast imaging, Software environment, Mathematical modeling.

DOI: [10.21272/jnep.15\(4\).04037](https://doi.org/10.21272/jnep.15(4).04037)

PACS numbers: 07.05.Pj, 87.64.mh, 42.30.Wb
87.59.e, 07.05.Wr, 29.50.v

1. INTRODUCTION

Non-destructive imaging plays a crucial role in such areas as health diagnostics, quality control of internal characteristics of food products, complex materials, and devices, analysis of cultural heritage items, transport security systems, etc. The most widely used of its methods is X-ray, which is characterized by high penetrating power and, therefore, the ability to reproduce both flat (2D) and three-dimensional (3D) three-dimensional information. The corresponding 3D imaging modality, computed tomography (CT), uses special reconstruction algorithms for this purpose. X-ray phase-contrast (XPC) imaging is a group of approaches that has been actively developing over the past few decades and is based on the phenomenon of refraction of X-rays (alternatively to the traditional absorption-based method) and the use of coherent radiation to obtain contrast images of the internal structure of low-absorbing or samples that contain functional materials with close atomic numbers, as in reactor solid fuel applications [1].

There are several experimental realizations of XPC, an important place among which is occupied by propagation-based XPC (PBXPC), when special optical elements (such as X-ray crystals, gratings, mirrors, masks, diffusers, which appear in other modalities [2-6]) are absent. However, in addition to the coherent radiation source inherent in other approaches, PBXPC relies on high requirements for spatial coherence and a high-resolution scintillation detector, both in systems with lens coupling and in systems with direct connection to solid-

state light detectors [7]. In this case, an important difference from the traditional absorption-based method, in which the distance between the sample and the detector is minimal, is the inherent propagation distance between the sample and the detector, i.e., the free space in which the phase of the wavefront generates intensity variations that are recorded in the experiment.

In the X-ray range, evolved and at the same time compact, regarding synchrotron facilities (ESRF, APS, Spring-8, ANSTO, etc.) with ultra-high brightness and intensity, are Compton sources, in which an infrared laser collides with accelerated electrons to produce X-rays (15-35keV). This project was implemented at the Munich Institute of Biomedical Engineering (MuCLS) and such a light source is known as a mini-synchrotron, which covers an area of $3 \times 5 \text{ m}^2$ [8].

Another advanced and progressive technology was the invention of a liquid-metal anode [9] as an X-ray source (8-22 keV), which allows for achieving a brightness of 10^{11} ph/sec, but in combination with Montel focusing mirrors that increase the density and maintain the uniformity of the flux [10]. An anode of this type is constantly regenerated and, therefore, increases the power of the source, compared to a conventional solid metal anode, for which the surface temperature of the surface in contact with the X-ray generating surface must not reach the melting point.

The first-of-its-kind integration of a Talbot-Lau interferometer (using three optical gratings between the source and detector) into a clinical CT gantry designed

* polishukav@ipfcentr.sumy.ua

for human medical diagnostics and, at the same time, its implementation in a CT radiochemical scanner should be highlighted [11]. The registered signal contains additional information about microstructural properties, especially in the case of lung tissue, which is permeated with a thin network of vessels and capillaries, and which are beyond the resolution of conventional CT systems, which is especially important for the diagnosis of various lung diseases. The information provided by this imaging modality is obtained by registering the so-called small-angle scattering [12], which, in turn, is provided by perfect (with a high aspect ratio > 100) X-ray gratings and their special inverse geometry [13].

Due to the need to process the data registered during an experiment (in the case of CT and especially in 4D time-series studies, such data volumes can reach tens of terabytes), there is a need for efficient algorithms for their processing, transformation, and display. This paper aims to semi-automate the search for the subjectively most contrast image among a dataset of images based on estimates of proximity to a given reference image.

Four commonly used metrics were utilized to quantify quality. The computer code and graphical user interface that we developed were used to determine the normalized picture and search for the image with the optimal contrast. The experimental data were the results of PBPCX biovisualization obtained at the undulator beamline NANOSCOPIUM of the synchrotron source SOLEIL [14] and were transmitted to us for processing and analysis.

The goal of this work is to investigate and apply numerical techniques to evaluate the quality of post-processed digital images acquired in present synchrotron and coming XPC studies using a quasi-monochromatic X-ray radiation source based on an electrostatic charged particle accelerator ‘‘Sokol’’[15].

2. MODEL AND METHODS

One of the basic stages in XPC for quantitative analysis is the phase retrieval [16] technique, in which the contrast of the images obtained in experiments is provided by the coherent characteristics of the radiation

source. Normalization of radiograms [17] is one of the necessary steps to obtain an undistorted and artifact-free image of the internal structure of the sample in XPC imaging.

A normalized image is:

$$I_{norm}(x, y) = \frac{I(x, y)}{I_0(x, y)} = \frac{S_{obj}(x, y) - S_{dark}(x, y)}{S_{flat}(x, y) - S_{dark}(x, y)},$$

where $S_{obj}(x, y)$ is an imaging (registered on the detector) signal when an object is present in the path of the probing X-rays; $S_{dark}(x, y)$ is a so-called ‘‘dark’’ signal when none of the X-ray photons hits the detector (the X-ray source is turned off); $S_{flat}(x, y)$ is the signal on the detector when there is no object in the path of X-rays; $I(x, y)$ and $I_0(x, y)$ are the phase-contrast intensity distributions in the detector plane with and without an object in front of it, respectively.

In Fig.1 $S_{flat}(x, y)$ and $S_{obj}(x, y)$ are the experimental nonuniform signals of the probing beam and of the insect wing are presented. However, without a suitable model and experimental data pre-processing, the quantitative analysis gives incorrect results. Fig. 2 demonstrates the phase retrieval using three models implemented in the software package PITRE [18] of the interaction of X-rays with the sample substance, substance as well as the method of their propagation namely: the Bronnikov modification, the single-material approximation, and the Fourier method in the first Born approximation [19]. The chosen models were designed by their authors to account for some known experimental details about imaging conditions and an optical path of radiation, like materials or substances in the imaged object or underlying scattering theory that describe the changes in intensity and corresponding direction. In this manner, various research groups have developed software packages [17-22], sometimes open-source [17, 21, 22], for image processing and quantitative analysis of XPC measurements.

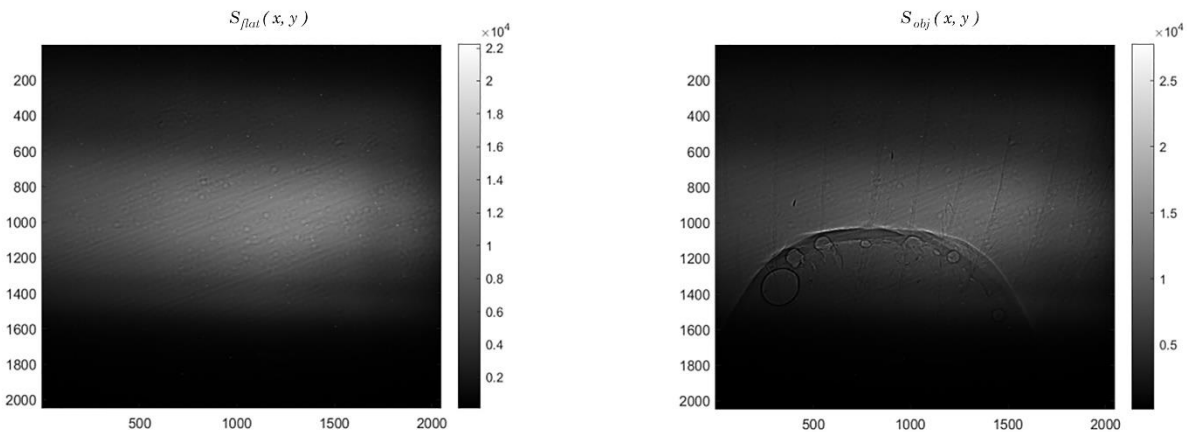


Fig. 1 – Registered experimental PBXPC signals (two out of three) of an insect wing which are input in the radiogram normalization procedure. Left and bottom axis indicate the position of the pixel. The scale on the right displays intensity in arb.u.

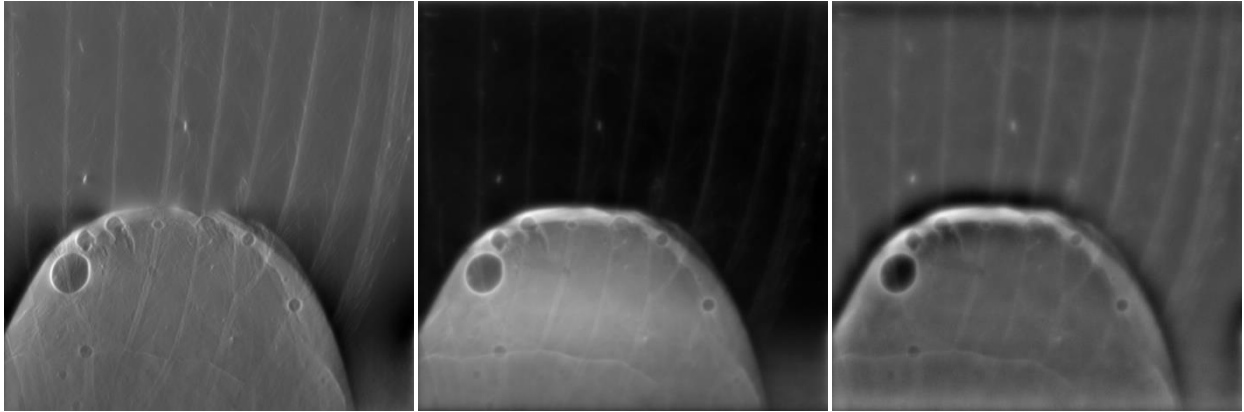


Fig. 2 – Phase retrieval using three models. Recovery parameters for: 1) the Bronnikov modification – $\gamma = 10^3$; 2) the single-material approximation – $\gamma = 10^2$; 3) the Fourier method in the first Born approximation – $\gamma = 10^4$ and an inherent regularization parameter α was set to 10^{-5}

Matlab was chosen for normalization [23]. Cloud computing in Matlab (via a web browser) was recently introduced; however, this tool needs Internet access but does not require any configuration or installation of the environment. On the contrary, by installing the application, you can profit from faster, more labor-intensive computations. Also, this resource allows you to use four common mathematical criteria (MS-SSIM, IMMSE, PNSR, SSIM) of image quality to assess deviations from the reference image.

In general, the task was implemented in the Matlab software product and packaged in our custom interface, shown in Fig. 3.

The algorithm of the program is as follows:

- 1) normalize and build the corrected image using three measured signals;
- 2) form the reference image by tuning the two parameters $[\alpha, \beta]$ and the increment (“Step”) by means of the interface;
- 3) run the reference-based numerical visual search to form a subsampling with the subjectively most contrast images.

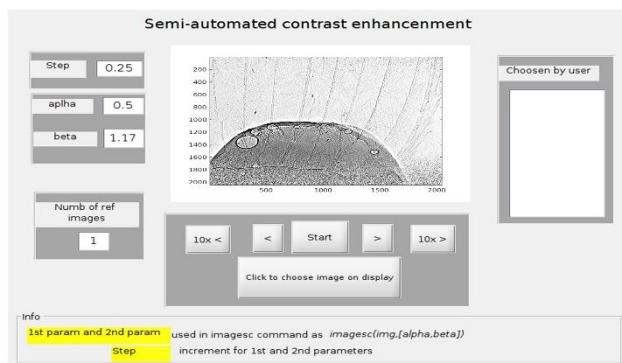


Fig. 3 – Interface for semi-automatic image contrast enhancement in the propagation-based X-ray phase contrast method

In such a manner our algorithm can generate thousands of images with variable contrast. Particular subsamples of images can then be used from such a dataset for numerical evaluation. We used mean square error (MSE), peak signal-to-noise ratio (PSNR), structural similarity index (SSIM), and multiscale structural simi-

larity index (MS-SSIM) as objective metrics for comparing the contrast between the reference and the given sample. However, our analysis is based only on PSNR and SSIM image quality metrics.

For two images $I(x, y)$ and $I'(x, y)$, the first of which is the reference image and the other is the compared image - PSNR is defined as:

$$PSNR = 10 \log_{10} \frac{MAX_{I(x,y)}^2}{MSE},$$

where $MAX_{I(x,y)}$ is the maximum possible pixel value for $I(x, y)$, and

$$MSE = \frac{1}{n} \sum [I(x, y) - I'(x, y)]^2,$$

where n – is the number of pixels in the image.

The PSNR depends on the MSE (mean square error), which in turn is responsible for pixel-by-pixel comparison. The IMMSE numerical criterion used in our research is identical to the conventional MSE. Additionally, for numerical evaluation, the measure of structural similarity (SSIM) index is considered and used

$$SSIM(x, y) = \frac{(2\mu_x\mu_y + c_1)(2\sigma_{xy} + c_2)}{(\mu_x^2 + \mu_y^2 + c_1)(\sigma_x^2 + \sigma_y^2 + c_2)},$$

where the subscripts x and y represent the reference and examined images, respectively, μ is the image average, σ is the image variation, and c_1, c_2 are constants.

3. RESULTS AND DISCUSSION

The object of visualization was a wing of a whitefly (family Aleyrodoidea), an insect pest of various agricultural vegetable and berry crops that are extremely important for human health growth. The projections of the wing were kindly provided to us as a result of experiments that were designed by a SOLEIL synchrotron source beamline scientist and corresponding data were collected at the micro-tomography end station. In this experiment, the energy of the undulator-based X-ray photons was 10 keV, the propagation distance (object-

detector) was set to 176 mm, and the detector (with indirect conversion) pixel size was 650 nm. The data were preformatted in Matlab.

The advantage of XPC imaging contrary to the traditional absorption approach, in the case of thin insect wing, is the inability of the commonly used absorption-based method to even slightly affect the attenuation and, consequently, to satisfactorily build a corresponding image. Hence, this state-of-the-art experimental PBXPC technique makes it available to us to study the structures on the cuticle and the position of its superimposed veins with high accuracy due to the inherent contrast sensitivity of the modality.

After we received the raw experimental images, it became necessary to reproduce them on the screen with optimal contrast. This goal was achieved by the manual selection of parameters. Thus, we decided to simplify this time-consuming step, and with this intention, we developed a program that helps speed up the subjective search for the most contrast image.

During the execution time of our developed program, a series of images were generated and stored into a sub-sampling of the images selected by us. From these images, one subjectively better than the others was manually selected, which we called the reference. This reference image is then mathematically compared with lots of variable contrast images that were generated by our program. The PSNR was used as a criterion that determines the pixel-by-pixel variations between the two given images, which are important factors for this work since the image of the wing is stationary and was not affected by additional distorting factors such as vibrations or other dynamical motions (in case of in vivo research) during the experiment. As an example, an image transformed by 90 degrees rotation will remain the same, but the PSNR will be much lower (PSNR = 12.3) in comparison to an image with each pixel simply magnified by a constant and without rotation (PSNR = 28.1). We confirm the fact, that the peculiarity of this metric is

its poor compatibility with visual, subjective assessment for general tasks because the PSNR quality metric is strongly dependent on the mean square deviation.

Another criterion we used for the analysis was the structural similarity (SSIM) index. This adaptive metric [24] usually combines and focuses on the estimation of contrast, brightness, and structural functions inherent in the image that allows for the adjustment of the respective component's input to the evaluation. As an example, in [25], SSIM was utilized as one of the image quality assessments in the visualization of overlapping vascular networks, where authors built an intermediate data synthesis model that allows them to reduce the required number of projections to lessen the radiation dose absorbed by the head using rotational radiography.

The reasoning behind using the chosen numerical metrics is that the more similar the given image being compared is to our chosen reference image, the greater the immediate value of the SSIM and the PSNR functions on the graph. In our case, the best option (visually selected reference image, with the pair of parameters $[\alpha, \beta] = [0.7, 1.17]$) from the partial sampling of the generated images were used for mathematical evaluation by the internal SSIM and PSNR algorithms to evaluate normalized images of the dataset (Fig. 4 and Fig. 5).

As a result, the absolute maxima in Figs. 4 and 5 are the most similar to the reference image for both numerical criteria and the values of the maxima near them are the images that the author gather into a collection of the best images during the semi-automatic selection process using the program.

And such algorithmic selection does take place and is analogous to the author's intuitive choice of the best-quality image. The susceptibility curve shown in Fig. 6 clearly demonstrates the similarity with the mathematical estimate when the algorithm reached the most similar images to the manually selected reference – that's when these similarity maxima in Fig. 4 and Fig. 5 were formed.

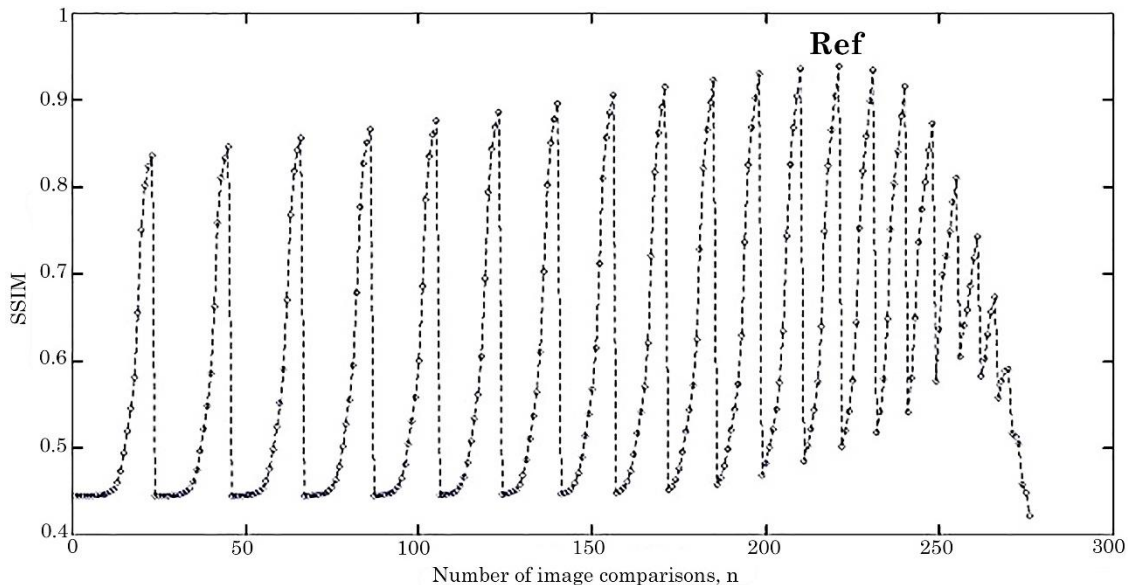


Fig. 4 – Numerical estimation of the similarity between the reference image and the images in the process of the dataset overrun by the SSIM criterion. **Ref** – is the image formed by $[\alpha, \beta]$ that is the closest in contrast to the reference image

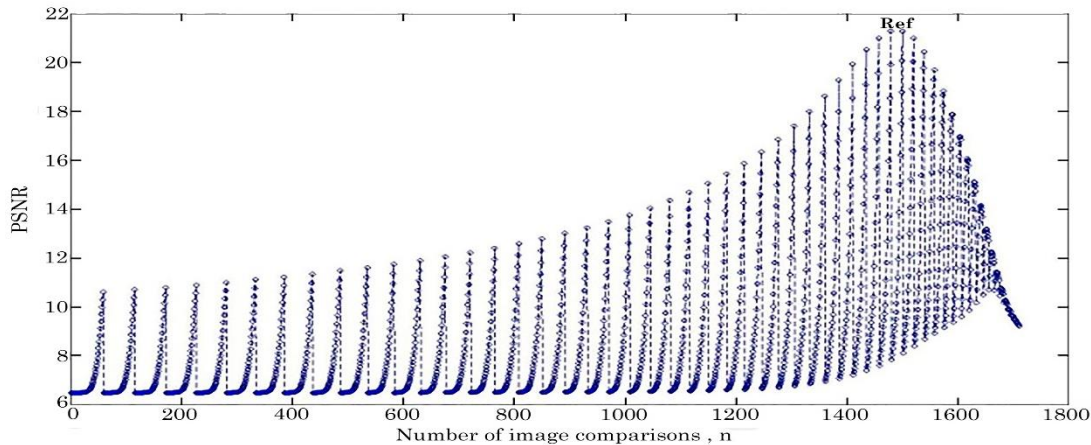


Fig. 5 – Numerical estimation of the contrast similarity between the reference image and the images in the process of the dataset overrun by the PSNR criterion. **Ref** – is the image formed by $[\alpha, \beta]$ pair that is the closest in contrast to the reference image

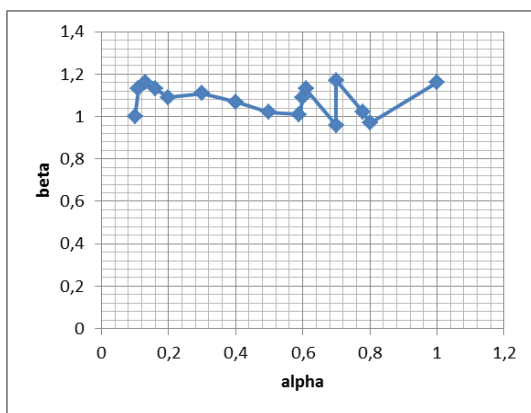


Fig. 6 – The author's susceptibility curve

4. CONCLUSIONS

Although X-ray image normalization was initiated a long time ago and implemented in software [18-20], its importance for this work is assessed both by the correct application of the known normalization algorithm and the one developed in this work for the subsequent displaying of a normalized image with optimal contrast based on an algorithmic comparison of the sample image with a visually perceptible reference. During the research, we created an in-house developed program that allows us to evaluate, according to commonly used quality criteria, the degree of similarity to a given contrast image selected by the researcher and select a reference image for numerical comparison.

Experimental data from an imaging experiment of an insect wing, obtained with the help of the SOLEIL synchrotron source, were given over to us via the Internet. The results of our processing and analysis of the experimental data became the developed interface and metric evaluation based on the reference for more convenient visual numerical control of the image contrast. During the research, we created an in-house developed

program that allows one to evaluate, according to commonly used quality criteria, the degree of similarity of a sample image from the dataset to a given contrast image selected by the researcher and, additionally, select a reference image for numerical comparison. The peak indicators of the chosen quality metrics help us to form a subsampling of images with optimal contrast, which in turn depends on a given reference image. The performed phase retrieval additionally requires quantitative analysis. During the study, a dataset with at least 6,500 images with a total volume of 2.5 GB was generated.

In the future, it is promising to use alternative metrics for numerical evaluation of quality improvement, particularly those that do not require a reference image or when some limited additional data about the visualized object is known. The benchmark approach used in this paper serves as a basis for further research for both subjective and objective mathematical criteria for image quality assessment as well as for developing non-reference automated methods, even though the effectiveness of the practical and skillful evaluation remains significant. The created program is a developed research product that may serve as a basis for automating the search and displaying of the most contrast 2D images represented in grayscale and, in particular, obtained by the PBXPC method; it supports not only *.mat files format but also plain text files which is also common for measurements. Such automated, algorithmic, and decision-making based on objective numerical estimates is a promising task for applying artificial intelligence to retrieve the optimal contrast images obtained in XPC experiments.

ACKNOWLEDGEMENTS

The authors are grateful to I. Protsenko for fruitful discussions and comments; K. Medjoubi (France, SOLEIL) for providing experimental data for their processing and analysis; O. Kulment'ev and V. Storizhko for help and valuable advice; A. Burvall and A. Rack for private correspondence.

REFERENCES

1. S. C. Mayo, A. W. Stevenson, S. W. Wilkins, *Mat.* **5**, 937 (2012).
2. T. Zhou, U. Lundström, T. Thüning, S. Rutishauser, D. H. Larsson, M. Stampanoni, C. David, H. M. Hertz, A. Burvall, *Opt. Express* **21**, 30183 (2013).
3. I. Zanette, T. Zhou, A. Burvall, U. Lundström, D. H. Larsson, M. -C. Zdora, P. Thibault, F. Pfeiffer, H. M. Hertz, *Phys. Rev. Lett.* **112**, 253903 (2014).
4. T. Zhou, I. Zanette, M. -C. Zdora, U. Lundström, D. H. Larsson, H. M. Hertz, F. Pfeiffer, A. Burvall, *Opt. Lett.* **40**, 2822 (2015).
5. I. Zanette, M. -C. Zdora, T. Zhou, A. Burvall, D. H. Larsson, P. Thibault, H. M. Hertz, F. Pfeiffer, *Proc. Natl. Acad. Sci. U. S. A.* **112**, 12569 (2015).
6. T. Zhou, I. Zanette, M. -C. Zdora, I. Zanette, J. Romell, H. M. Hertz, A. Burvall, *Opt. Lett.* **41**, 5490 (2016).
7. R. Gradl, M. Dierolf, B. Günther, L. Hehn, W. Möller, D. Kutschke, L. Yang, M. Donnelly, R. Murrie, A. Erl, T. Stoeger, B. Gleich, K. Achterhold, O. Schmid, F. Pfeiffer, K. Morgan, *Sci. Rep.* **8**, 6788 (2018).
8. B. Gunther, R. Gradl, C. Jud, E. Eggl, J. Huang, S. Kulpe, K. Achterhold, B. Gleich, M. Dierolf, F. Pfeiffer, *J. Synchrotron Rad.* **27**, 1395 (2020).
9. O. Hemberg, M. Otendal, and H. M. Hertz, *Appl. Phys. Lett.* **83**, 1483 (2003).
10. M. Montel, *X ray Microsc. and Microrad.* **57-11935**, 177 (1957).
11. M. Viermetz, N. Gustschin, C. Schmid, J. Haeusele, M. von Teuffenbach, P. Meyer, F. Bergner, T. Lasser, R. Proksa, T. Koehler, F. Pfeiffer, *PNAS*, Vol. **119**, No. **8** (2022).
12. W. Yashiro, Y. Terui, K. Kawabata, A. Momose, *Opt. Express* **18**, 16890 (2010).
13. T. Donath, M. Chabior, F. Pfeiffer, O. Bunk, E. Reznikova, J. Mohr, E. Hempel, S. Popescu, M. Hoheisel, M. Schuster, J. Baumann, C. David, *J. Appl. Phys.* **106**, 054703 (2009).
14. K. Medjoubi, G. Baranton, A. Somogyi, *Microsc. Microanal.* **24**(Suppl. 2), 252 (2018).
15. O. M. Buhay, A. A. Drozdenko, M. I. Zakharets, I. G. Ignat'ev, A. B. Kramchenkov, V. I. Miroshnichenko, A. G. Ponomarev, V. E. Storizhko, *Phys. Procedia* **66**, 166 (2015).
16. D. Paganin, D. Pelliccia <https://arxiv.org/abs/1902.00364>.
17. T. Weitkamp, D. Haas, D. Wegrzynek, A. Rack, *J. Synchrotron Rad.* **18**, 617 (2011).
18. R. -C. Chen, D. Dreossi, L. Mancini, R. Menk, L. Rigon, T. -Q. Xiao, R. Longo, *J. Synchrotron Rad.* **19**, 836 (2012).
19. A. Burvall, U. Lundström, P. Takman, D. Larsson, H. Hertz, *Opt. Express* **19**, 10359 (2011).
20. T. Gureyev, Y. Nesterets, D. Ternovski, D. Thompson, S. Wilkins, A. Stevenson, A. Sakellariou, J. Taylor, *Proc. of SPIE Vol. 8141*, No. **81410B** (2011).
21. F. Brun, L. Massimi, M. Fratini, D. Dreossi, F. Billé, A. Accardo, R. Pugliese, A. Cedola, *Adv. Struct. Chem. Imag.* **3**, No. **4** (2017).
22. A. Bergamaschi, K. Medjoubi, C. Messaoudi, S. Marco, A. Somogyi, *J. Synchrotron Rad.* **23**, 783 (2016).
23. Matlab-online, <https://matlab.mathworks.com/>
24. Z. Wang, H. Sheikh, *IEEE Trans. Image Process.* Vol. **13**, No. **4** (2004).
25. T. Siow, C. -Y. Ma, C. H. Toh, *Biomed. J.* (2022).

Інтерфейс напівавтоматичного покращення контрастності зображень у рентгенівському фазовому контрасті на основі вільного поширення

А.В. Поліщук¹, М.О. Павлюк^{1,2}, А.В. Тарасенко², В.В. Журакулов²

¹ Інститут прикладної фізики НАН України, вул. Петропавлівська, 58, 40000 Суми, Україна

² Сумський державний університет, вул. Римського-Корсакова, 2, 40007 Суми, Україна

У роботі описується графічний інтерфейс користувача, розроблений для нормалізації радіограм та напівавтоматичного пошуку контрастних зображень за допомогою заданого еталону, експериментальні дані для формування яких були отримані за допомогою аналітичної техніки рентгенівського фазового контрасту. Проекції біологічного об'єкта були одержані шляхом застосування вільного поширення когерентного випромінювання, коли для використання інтерференційних ефектів, характерних методу, між зразком та детектором, оснащеним YAG:Ce скінтілятором, не розміщуються жодні допоміжні оптичні елементи завдяки високоінтенсивним характеристикам рентгенівського світла синхротронного джерела SOLEIL. Енергія рентгенівських фотонів була 10 keV, а відстань між зразком та детектором становила 16.5 см. Розглядається застосування стандартних інструментів середовища Matlab для алгоритмічної корекції неоднорідностей детектора і зондувальних променів світла, використаних щоб побудувати зображення внутрішньої структури об'єкту та для оцінювання контрастності групи зображень, обравши такі поширені критерії як PSNR та SSIM. Програма здатна генерувати такий набір зображень в залежності від параметрів, які вводить користувач для суб'єктивного пошуку контрастних зображень. Чисельні оцінки добре підтверджують візуальні результати алгоритмічного перебору та дозволяють отримати найінформативніше зображення з утвореного масиву, який створюється користувачем за допомогою інтерфейсу. Робота переслідує мету ознайомити з використанням розробленого програмного продукту та концепту напівавтоматичного перебору цифрових фазо-контрастних зображень.

Ключові слова: Матлаб, Напівавтоматика, Інтерфейс, Нормалізація, Рентгенівський фазовий контраст, Програмне середовище, Математичне моделювання.